Numer Algor (2013) 63:143–164
DOI 10.1007/s11075-012-9617-3

ORIGINAL PAPER

Analysis for one-dimensional time-fractional Tricomi-type equations by LDG methods

Xindong Zhang · Juan Liu · Juan Wen · Bo Tang · Yinnian He

Received: 13 November 2011 / Accepted: 26 June 2012 /
Published online: 13 July 2012

Abstract In this paper, we consider the local discontinuous Galerkin (LDG) finite element method for one-dimensional linear time-fractional Tricomi-type equation (TFTTE), which is obtained from the standard one-dimensional linear Tricomi-type equation by replacing the first-order time derivative with a fractional derivative (of order α, with $1 < \alpha \leq 2$). The proposed LDG is based on LDG finite element method for space and finite difference method for time. We prove that the method is unconditionally stable, and the numerical solution converges to the exact one with order $O(h^{k+1} + \tau^2)$, where h, τ and k are the space step size, time step size, polynomial degree, respectively. The comparison of the LDG results with the exact solutions is made, numerical experiments reveal that the LDG is very effective.

This work is supported by the Key Project of Chinese Ministry of Education (211202), the NSF of China (Nos. 10971166 and 61163027) and the National High Technology Research and Development Program of China (863 Program, No. 2009AA01A135).

X. Zhang (✉) · Y. He
College of Mathematics and System Sciences, Xinjiang University,
Urumqi, Xinjiang, 830046, People's Republic of China
e-mail: liaoyuan1126@163.com

X. Zhang · J. Liu
College of Mathematics Sciences, Xinjiang Normal University,
Urumqi, Xinjiang, 830054, People's Republic of China

J. Wen · B. Tang · Y. He
Center for Computational Geosciences, School of Mathematics and Statistics,
Xi'an Jiaotong University, Xi'an, Shanxi, 710049, People's Republic of China

Keywords Linear time-fractional Tricomi-type equation · Local discontinuous Galerkin finite element method · Caputo fractional derivative · Fractional differential equation

1 Introduction

Fractional differential equations (FDEs) is considered as the generalization of the classical (or integer order) differential with a history of at least three hundred years. It can be dated back to Leibniz's letter to L'Hospital, in which the meaning of the one-half order derivative was first discussed [1]. Although it has such a long history, its research still stay in the realm of theory, due to the lack of proper mathematical analysis methods and real applications. However, the use of FDEs in mathematical models has become increasingly popular in recent years. Different models using FDEs have been proposed in more and more fields, such as in viscoelastic mechanics, power-law phenomenon in fluid and complex network, allometric scaling laws in biology and ecology, electromagnetic waves, quantum evolution of complex systems, and so on. For example, the nonlinear oscillation of earthquake can be modeled with fractional derivatives [2], and the fluid-dynamic traffic model with fractional derivatives [3] can eliminate the deficiency arising from the assumption of continuum traffic flow. On the basis of experimental data, fractional partial differential equations for seepage flow in porous media are suggested in [4]. A review of some applications of fractional derivatives in continuum and statistical mechanics is given by Mainardi [5].

FDEs gain the advantage over the classical one in modeling some materials with memory, heterogeneity or inheritable character. Most of the FDES cannot be solved exactly, approximate and numerical methods must be used. The modeling progress on using FDEs has led to increasing interest in developing numerical schemes for their solutions. Several methods have been introduced to solve FDEs and differential equations, the popular Laplace transform method [1, 6], the spline collocation method [7], the finite difference/spectral method [8–16], the Fourier transform method [17], the iteration method [18] and the operational method [19], the homotopy perturbation/analysis method [20–28], and so on.

In the present paper we use the LDG to construct the numerical solution to Tricomi-type equation with time-fractional derivatives of the form,

$$\begin{cases} D_t^{\alpha} u(x,t) - t^{2\kappa} \Delta u(x,t) = f(x,t), \quad (x,t) \in \Omega \times [0,T], \\ u(x,t)\,|_{t=0} = u_0(x), \ \dfrac{\partial u(x,t)}{\partial t}\,|_{t=0} = u_1(x), \ x \in \Omega = [a,b], \end{cases} \tag{1}$$

where $1 < \alpha \leq 2$, κ is a real non-negative number, $D_t^{\alpha} := \frac{\partial^{\alpha}}{\partial t^{\alpha}}$ (defined as Definition 1.1) denotes the Caputo fractional derivatives in time and $f(x,t)$ is given function. Δ is the differential operator

$$\Delta u(x,t) := \frac{\partial^2 u(x,t)}{\partial x^2} = u_{xx}.$$

When $\alpha = 2, \kappa = 1/2$ and $f(x,t) \equiv 0$, (1) is the linear Tricomi equation. This is why (1) is said to be of Tricomi-type. In 1923, Tricomi [29] initiated work on boundary value problems for a linear partial differential operator of mixed type and related equations of variable type (for $t > 0$ the Tricomi equation is hyperbolic, while for $t < 0$ it is elliptic). In 1945, Frankl [30] drew attention to the fact that the Tricomi problem was closely connected to the study of gas flows with nearly sonic speeds. More precisely, the Tricomi equation describes the transition from subsonic flow (elliptic region) to supersonic flow (hyperbolic region). In [31–35] one can find more about applications of the Tricomi equation. For $\alpha = 2$, the motivation to investigate the problem for (1) comes from physical problems of gas dynamics [31].

In this paper, we aim to effectively employ the LDG method to establish the numerical solutions for (1). The discontinuous Galerkin (DG) method has several attractive properties. First, it can be easily designed for any order of accuracy. Meanwhile, since the order of accuracy can be locally determined in each cell independently, it is flexible for arbitrary p adaptivity. Second, we can use arbitrary triangulations even those with hanging nodes, which is different from the traditional finite element method. So arbitrary h adaptivity is allowed. Third, Since the solution in each cell needs to communicate only with the immediate neighbors, the method has excellent parallel efficiency. Finally, we can prove its nonlinear stability results easily by choosing the numerical fluxes carefully. Discontinuous Galerkin methods are a class of finite element methods using completely discontinuous basis functions, which are usually chosen as piecewise polynomials. Since the basis functions can be completely discontinuous, these methods have the flexibility which is not shared by typical finite element methods. The first DG method was introduced in 1973 by Reed and Hill [36], in the framework of neutron transport, i.e. a time independent linear hyperbolic equation. A major development of the DG method is carried out by Cockburn et al. in a series of papers [37–40]. It is difficult to apply the DG method directly to the equations with higher order derivatives. This is because the solution space, which consists of piecewise polynomials discontinuous at the element interfaces, is not regular enough to handle higher derivatives. The idea of LDG methods for time dependent partial differential equations with higher derivatives, is to rewrite the equation into a first order system, then apply the DG method on the system. A key ingredient for the success of such methods is the correct design of interface numerical fluxes. These fluxes must be designed to guarantee stability and local solvability of all the auxiliary variables introduced to approximate the derivatives of the solution. The first LDG method was developed by Cockburn and Shu [41], for the convection diffusion equation containing second derivatives. The local solvability of all the auxiliary variables is why the method is called a "local" DG method in [41]. The LDG method has been successfully applied to solve many types of linear and nonlinear problems in science and engineering by many authors [42–53] and also been used to solve fractional differential equations [54].

Definition 1.1 [6] The fractional derivative in the Caputo sense of $u(t) \in C_{-1}^{m}, m \in N, t > 0$ is defined as

$$D_t^{\alpha} u(t) = \begin{cases} \dfrac{1}{\Gamma(m-\alpha)} \int_0^t u^m(s) \dfrac{ds}{(t-s)^{1+\alpha-m}} & \text{for } m-1 < \alpha < m, \\ \dfrac{d^m}{dt^m} u(t) & \text{for } \alpha = m, \end{cases} \tag{2}$$

where $\Gamma(\bullet)$ is the Gamma function.

2 The LDG method for one-dimensional TFTTEs

As before, we assume that the following mesh to cover the computational domain $\Omega = [a, b]$, consisting of cell $I_i = [x_{i-\frac{1}{2}}, x_{i+\frac{1}{2}}]$, for $1 \le i \le M$, where $a = x_{\frac{1}{2}} < x_{\frac{3}{2}} < \cdots < x_{N+\frac{1}{2}} = b$. We denote $\Delta x_i = x_{i+\frac{1}{2}} - x_{i-\frac{1}{2}}$, $1 \le i \le M; h = \max_{1 \le i \le M} \Delta x_i$. And denote by $u_{i+\frac{1}{2}}^{+}$ and $u_{i+\frac{1}{2}}^{-}$ the values of u at $x_{i+\frac{1}{2}}$, respectively, from the right cell I_{i+1} and from the left cell I_i. $[u]_{i+\frac{1}{2}} = u_{i+\frac{1}{2}}^{+} - u_{i+\frac{1}{2}}^{-}$ denotes the jump of the function u at the cell interfaces.

We define a finite element space consisting of piecewise polynomials

$$V_h^k = \{v : v|_{I_i} \in P^k(I_i),\ 1 \le i \le M\}, \tag{3}$$

where $P^k(I_i)$ denotes the set of polynomials of degree up to k defined on the cell I_i. In order to prove the convergence of the scheme, we need the projections $\mathbb{P}$ and $\mathbb{P}^{\pm}$ in $[a, b]$, such that for each i,

$$\begin{aligned} &\int_{I_i} (\mathbb{P}\omega(x) - \omega(x)) v(x) dx = 0,\ \forall v \in P^k(I_i); \\ &\int_{I_i} (\mathbb{P}^{+}\omega(x) - \omega(x)) v(x) dx = 0,\ \forall v \in P^{k-1}(I_i) \text{ and } \mathbb{P}^{+}\omega\left(x_{i-\frac{1}{2}}^{+}\right) = \omega\left(x_{i-\frac{1}{2}}\right); \\ &\int_{I_i} (\mathbb{P}^{-}\omega(x) - \omega(x)) v(x) dx = 0,\ \forall v \in P^{k-1}(I_i) \text{ and } \mathbb{P}^{-}\omega\left(x_{i+\frac{1}{2}}^{-}\right) = \omega\left(x_{i+\frac{1}{2}}\right). \end{aligned} \tag{4}$$

Notice that these projections are used in the error estimates of the LDG methods to derive optimal L^2 error bounds in the literature. There are some approximation results for the projections [42, 46]

$$\|\omega^e\| + h\|\omega^e\|_{\infty} + h^{\frac{1}{2}}\|\omega^e\|_{\tau_h} \le C_u h^{k+1}, \tag{5}$$

where $\omega^e = \mathbb{P}\omega - \omega$ or $\omega^e = \mathbb{P}^{\pm}\omega - \omega$. Here and below C_u (which may not have the same value in different places) is a generic constant depending on u and its derivatives but independent of h. τ_h denotes the set of boundary points of all elements I_i. We use C depending on u, T and α to denote a positive constant which may have a different value in each occurrence. The norm $\|\bullet\|$ denotes the L^2 norm on Ω.

In order to introduce the numerical scheme for the solution of (1), we need to divide the time space into N cells, where N is a positive integer. Let $t_n := n\tau$, where $\tau := T/N$ is the time step, $n = 0, 1, \cdots, N$ be mesh points. The time-fractional derivative $D_t^\alpha u(x, t_n)$ at t_n is estimated in [55] as following

$$D_t^\alpha u(x,t_n) = \frac{\tau^{-\alpha}}{\Gamma(3-\alpha)} \sum_{j=1}^{n} b_{n-j}(u(x,t_j) - 2u(x,t_{j-1}) + u(x,t_{j-2})) + E_\tau^{(n)}(x), \tag{6}$$

where $b_{n-j} = (n-j+1)^{2-\alpha} - (n-j)^{2-\alpha} > 0$ and $1 = b_0 > b_1 > b_2 > \cdots > b_n = 0$ as $n \to \infty$. In particular, for $j = 1$, denote $u(x, t_{-1}) \approx u^{-1} = u(x, 0) - \tau u'(x, 0) = u_0(x) - \tau u_1(x)$.

As analysis in [55], we can get the following lemma.

Lemma 2.1 [55] *The truncation error $E_\tau^{(n)}(x)$ defined by (6) is bounded by*

$$\| E_\tau^{(n)}(x) \| \le \frac{C M_1 T^{2-\alpha}}{\Gamma(3-\alpha)} \tau + o(\tau^2) \le C\tau, \tag{7}$$

where M_1 is the upper bound of $|\frac{\partial^3}{\partial t^3} u(x,t)|$ and C is a constant depending on u, T and α.

The LDG scheme is formulated based on rewriting (1) into a first-order system,

$$\begin{cases} D_t^\alpha u(x,t) - t^{2\kappa} q_x = f(x,t), \\ q - u_x = 0. \end{cases} \tag{8}$$

Let u_h^{-1}, u_h^n and q_h^n be the approximation of u^{-1}, $u(x, t_n)$ and $q(x, t_n)$, respectively. And let $f^n = f(x, t_n)$. First, we can get the weak form of (1) at t_1 by (6) and (8),

$$\begin{cases} \int_\Omega u(x,t_1) v dx + \lambda\beta \left\{ \int_\Omega q(x,t_1) v_x dx - \sum_{i=1}^{M} \left[(q(x,t_1)v^-)_{i+\frac{1}{2}} - (q(x,t_1)v^+)_{i-\frac{1}{2}} \right] \right\} \\ = 2\int_\Omega u(x,t_0) v dx - \int_\Omega u(x,t_{-1}) v dx - \beta \int_\Omega E_\tau^{(1)}(x) v dx + \beta \int_\Omega f^1 v dx; \\ \int_\Omega q(x,t_1)\omega dx + \int_\Omega u(x,t_1)\omega_x dx - \sum_{i=1}^{M} \left\{ (u(x,t_1)\omega^-)_{i+\frac{1}{2}} - (u(x,t_1)\omega^+)_{i-\frac{1}{2}} \right\} = 0, \end{cases} \tag{9}$$

For $n = 1$, the fully discrete local discontinuous Galerkin scheme becomes: find $u_h^1, q_h^1 \in V_h^k$, such that

$$\begin{cases} \int_\Omega u_h^1 v dx + \lambda\beta \left\{ \int_\Omega q_h^1 v_x dx - \sum_{i=1}^{M} \left[\left(\widehat{q_h^1} v^-\right)_{i+\frac{1}{2}} - \left(\widehat{q_h^1} v^+\right)_{i-\frac{1}{2}} \right] \right\} \\ = 2\int_\Omega u_h^0 v dx - \int_\Omega u_h^{-1} v dx + \beta \int_\Omega f^1 v dx; \\ \int_\Omega q_h^1 \omega dx + \int_\Omega u_h^1 \omega_x dx - \sum_{i=1}^{M} \left\{ \left(\widehat{u_h^1}\omega^-\right)_{i+\frac{1}{2}} - \left(\widehat{u_h^1}\omega^+\right)_{i-\frac{1}{2}} \right\} = 0, \end{cases} \tag{10}$$

hold for any $v, \omega \in V_h^k$.

Next, we can get the weak form of (1) at t_n by (6) and (8) for $n = 2, 3, \cdots, N$,

$$\begin{cases} \int_\Omega u(x,t_n)vdx + \lambda\beta\{\int_\Omega q(x,t_n)v_x dx - \sum_{i=1}^{M}[(q(x,t_n)v^-)_{i+\frac{1}{2}} - (q(x,t_n)v^+)_{i-\frac{1}{2}}]\} \\ = \sum_{j=2}^{n-1}(-b_j + 2b_{j-1} - b_{j-2})\int_\Omega u(x,t_{n-j})vdx + (2b_{n-1} - b_{n-2})\int_\Omega u(x,t_0)vdx \\ - b_{n-1}\int_\Omega u(x,t_{-1})vdx + (2b_0 - b_1)\int_\Omega u(x,t_{n-1})vdx - \beta\int_\Omega E_\tau^{(n)}(x)vdx \\ + \beta\int_\Omega f^n vdx; \\ \int_\Omega q(x,t_n)\omega dx + \int_\Omega u(x,t_n)\omega_x dx - \sum_{i=1}^{M}\left\{(u(x,t_n)\omega^-)_{i+\frac{1}{2}} - (u(x,t_n)\omega^+)_{i-\frac{1}{2}}\right\} = 0. \end{cases} \tag{11}$$

Then the fully discrete local discontinuous Galerkin scheme becomes: find $u_h^n, q_h^n \in V_h^k$, such that

$$\begin{cases} \int_\Omega u_h^n vdx + \lambda\beta\left\{\int_\Omega q_h^n v_x dx - \sum_{i=1}^{M}\left[\left(\widehat{q_h^n}v^-\right)_{i+\frac{1}{2}} - \left(\widehat{q_h^n}v^+\right)_{i-\frac{1}{2}}\right]\right\} \\ = \sum_{j=2}^{n-1}(-b_j + 2b_{j-1} - b_{j-2})\int_\Omega u_h^{n-j}vdx + (2b_{n-1} - b_{n-2})\int_\Omega u_h^0 vdx \\ -b_{n-1}\int_\Omega u_h^{-1}vdx + (2b_0 - b_1)\int_\Omega u_h^{n-1}vdx + \beta\int_\Omega f^n vdx; \\ \int_\Omega q_h^n\omega dx + \int_\Omega u_h^n\omega_x dx - \sum_{i=1}^{M}\left\{\left(\widehat{u_h^n}\omega^-\right)_{i+\frac{1}{2}} - \left(\widehat{u_h^n}\omega^+\right)_{i-\frac{1}{2}}\right\} = 0, \end{cases} \tag{12}$$

hold for any $v, \omega \in V_h^k$. Where $\lambda = (n\tau)^{2\kappa}$, $\beta = \tau^\alpha\Gamma(3-\alpha)$.

The "hat" terms in (12) in the cell boundary terms from integration by parts are the so-called "numerical fluxes", in order to ensure stability, the alternating fluxes can be chosen as

$$(a):\ \widehat{u_h^n} = (u_h^n)^-,\ \widehat{q_h^n} = (q_h^n)^+ \ \text{ or } \ (b):\ \widehat{u_h^n} = (u_h^n)^+,\ \widehat{q_h^n} = (q_h^n)^-. \tag{13}$$

We remark that the choice for the fluxes (13) is not unique. In fact the crucial part is taking $\widehat{u_h^n}$ and $\widehat{q_h^n}$ from opposite sides. About the "numerical fluxes", one can refer [43, 56].

3 Stability analysis and error estimates of LDG

In order to simplify the notations and without loss of generality, we consider the case $f \equiv 0$ in stability analysis and error estimates. And the following Lemma 3.1 is needed.

Lemma 3.1 *Let* $u^{-1} = u(x,0) - \tau u'(x,0) = u_0(x) - \tau u_1(x)$ *and* $e^{-1} = u(x,t_{-1}) - u^{-1}$, *then*

$$|e^{-1}| \le C_u\tau^2 \text{ and } \|u_h^{-1}\| \le C_u(\|u_h^0\| + \tau\|u_1(x)\|), \tag{14}$$

in which C_u *is a constant depending on u.*

Proof We first show that $|e^{-1}| \le C_u\tau^2$. By the definition of e^{-1} and using Taylor expansion, we get that

$$|e^{-1}| = |u(x,t_{-1}) - u^{-1}| = |u(x,t_{-1}) - u(x,0) + \tau u'(x,0)|$$

$$= \frac{\tau^2}{2}u''(x,0) + o(\tau)^3 \le C_u\tau^2.$$

Next, we will show that $\|u_h^{-1}\| \le C(\|u_h^0\| + \tau\|u_1(x)\|)$. We know that

$$\int_\Omega u_h^{-1}vdx = \int_\Omega \mathbb{P}(u_0(x) - \tau u_1(x))vdx = \int_\Omega (u_h^0 - \tau u_1(x))vdx$$

hold for any $v \in V_h^k$. Taking $v = u_h^{-1}$ and by the fact $\int_\Omega uvdx \le \frac{1}{4}\|u\|^2 + \|v\|^2$, we can get that

$$\|u_h^{-1}\|^2 = \int_\Omega u_h^{-1}u_h^{-1}dx = \int_\Omega u_h^0u_h^{-1}dx - \int_\Omega \tau u_1(x)u_h^{-1}dx$$

$$\le \frac{1}{4}\|u_h^{-1}\|^2 + \|u_h^0\|^2 + \frac{1}{4}\|u_h^{-1}\|^2 + \tau^2\|u_1(x)\|^2,$$

therefore, we can obtain that

$$\|u_h^{-1}\| \le C_u(\|u_h^0\| + \tau\|u_1(x)\|), \tag{15}$$

where C is a constant depending on u, T and α. Then the lemma is proved. □

Let $e_u^{-1} = u(x,t_{-1}) - u_h^{-1}$. By the Lemma 3.1 and using the property (5), we can get the following result, which will be used in the proof of Theorem 3.3,

$$\|u(x,t_{-1}) - u_h^{-1}\| \le C_u(h^{k+1} + \tau^2). \tag{16}$$

For the fully discrete (10) for $n = 1$ and (12) for $n \ge 2$, we have the following stability result.

Lemma 3.2 *For periodic or compactly supported boundary conditions, the fully discrete LDG scheme* (12) *(*(10) *for* $n = 1$*) is unconditionally stable in the sense that for all* $\tau > 0$ *and* $h > 0$*, it holds*

$$\|u_h^n\| \le C(\|u_h^0\| + \tau\|u_1(x)\|), \ n = 1, 2, \cdots, N, \tag{17}$$

where C is a constant and depends on T, α *and u.*

Proof We only prove for the flux choice (13)-(b). If we use (13)-(a), the proof is similar and is thus omitted here.

If we take $v = u_h^n$, $\omega = \lambda\beta q_h^n$ and the flux as (13)-(b). For periodic or compactly supported boundary conditions, we can get that

$$\begin{aligned}
&\lambda\beta\left\{\int_\Omega q_h^n v_x dx - \beta\sum_{i=1}^{M}\left[\left(\widehat{q_h^n}v^-\right)_i - \left(\widehat{q_h^n}v^+\right)_{i-1}\right]\right\}\\
&\quad+\int_\Omega u_h^n\omega_x dx - \sum_{i=1}^{M}\left\{\left(\widehat{u_h^n}\omega^-\right)_i - \left(\widehat{u_h^n}\omega^+\right)_{i-1}\right\}\\
&=\lambda\beta\int_\Omega q_h^n(u_h^n)_x dx - \lambda\beta\sum_{i=1}^{M}\left[((q_h^n)^-(u_h^n)^-)_i - ((q_h^n)^-(u_h^n)^+)_{i-1}\right]\\
&\quad-\lambda\beta\int_\Omega q_h^n(u_h^n)_x dx + \lambda\beta\sum_{i=1}^{M}\left\{((q_h^n)^-(u_h^n)^-)_i - ((q_h^n)^+(u_h^n)^+)_{i-1}\right\}\\
&\quad-\lambda\beta\sum_{i=1}^{M}\left\{((u_h^n)^+(q_h^n)^-)_i - ((u_h^n)^+(q_h^n)^+)_{i-1}\right\}\\
&=\lambda\beta\sum_{i=1}^{M}\left\{((q_h^n)^-(u_h^n)^+)_{i-1} - ((u_h^n)^+(q_h^n)^-)_i\right\}\\
&=0.
\end{aligned}$$

Therefore, if we take $v = u_h^n$, $\omega = \lambda\beta q_h^n$ in (12) and the flux as (13)-(b), by simple computation, we can get that

$$\begin{aligned}
&\|u_h^n\|^2 + \lambda\beta\|q_h^n\|^2\\
&\quad=\sum_{j=2}^{n-1}(-b_j + 2b_{j-1} - b_{j-2})\int_\Omega u_h^{n-j}u_h^n dx + (2b_{n-1} - b_{n-2})\int_\Omega u_h^0 u_h^n dx\\
&\quad- b_{n-1}\int_\Omega u_h^{-1}u_h^n dx + (2b_0 - b_1)\int_\Omega u_h^{n-1}u_h^n dx.
\end{aligned}\tag{18}$$

We will prove the inequality (17) by induction. When $n = 1$, by (10) we have

$$\begin{cases}
\int_\Omega u_h^1 v dx + \lambda\beta\left\{\int_\Omega q_h^1 v_x dx - \sum_{i=1}^{M}\left[\left(\widehat{q_h^1}v^-\right)_{i+\frac{1}{2}} - \left(\widehat{q_h^1}v^+\right)_{i-\frac{1}{2}}\right]\right\}\\
\quad=\int_\Omega\left(2u_h^0 - u_h^{-1}\right)v dx;\\
\int_\Omega q_h^1\omega dx + \int_\Omega u_h^1\omega_x dx - \sum_{i=1}^{M}\left\{\left(\widehat{u_h^1}\omega^-\right)_{i+\frac{1}{2}} - \left(\widehat{u_h^1}\omega^+\right)_{i-\frac{1}{2}}\right\} = 0.
\end{cases}\tag{19}$$

Taking $v = u_h^1, \omega = \lambda\beta q_h^1$ in (19), by Lemma 3.1 and the fact $\int_\Omega uvdx \le \|u\|\|v\|$, we have

$$\|u_h^1\|^2 + \lambda\beta\|q_h^1\|^2 = \int_\Omega (2u_h^0 - u_h^{-1})u_h^1 dx \le (2\|u_h^0\| + \|u_h^{-1}\|)\|u_h^1\|,$$

which means that

$$\|u_h^1\| \le C(\|u_h^0\| + \|u_h^{-1}\|) \le C(\|u_h^0\| + \tau\|u_1(x)\|).$$

Assuming that $\|u_h^n\| \le C(\|u_h^0\| + \tau\|u_1(x)\|)$ holds for $n = J (J < N)$, we want to prove that it holds for $n = J + 1$. For $n = J + 1$, by (18) we get that

$$\|u_h^{J+1}\| \le \sum_{j=2}^{J} |-b_j + 2b_{j-1} - b_{j-2}|\|u_h^{J+1-j}\| + |2b_J - b_{J-1}|\|u_h^0\|$$

$$+ b_J\|u_h^{-1}\| + (2b_0 - b_1)\|u_h^J\|.$$

Using $b_0 = 1$, by Lemma 3.1 and the induction assumption, we obtain

$$\begin{aligned}
\|u_h^{J+1}\| &\le C\left(\sum_{j=2}^{J} |-b_j + 2b_{j-1} - b_{j-2}| + |2b_J - b_{J-1}| + b_J + 2 - b_1\right) \\
&\quad \times (\|u_h^0\| + \tau\|u_1(x)\|) \\
&\le C\left(\sum_{j=2}^{J} |b_{j-1} - b_j| + |b_{j-2} - b_{j-1}| + b_J + b_{J-1} + 2 - b_1\right) \\
&\quad \times (\|u_h^0\| + \tau\|u_1(x)\|) \\
&= 3C(\|u_h^0\| + \tau\|u_1(x)\|) = C(\|u_h^0\| + \tau\|u_1(x)\|),
\end{aligned}$$

and we are done. □

Next, we will present and prove the main convergence theorem.

Theorem 3.3 *Let $u(x, t_n)$ be the exact solution of (1) and u_h^n be the numerical solution of the fully discrete LDG scheme (12) ((10) for $n = 1$). Then*

$$\|u(x, t_n) - u_h^n\| \le C(h^{k+1} + \tau^2), \ n = 1, 2, \cdots, N, \tag{20}$$

where C is a constant and depends on T, α and u.

Proof We denote

$$\begin{cases} e_u^n = u(x,t_n) - u_h^n = \mathbb{P}^+ e_u^n - [\mathbb{P}^+ u(x,t_n) - u(x,t_n)], \\ e_q^n = q(x,t_n) - q_h^n = \mathbb{P}^- e_q^n - [\mathbb{P}^- q(x,t_n) - q(x,t_n)]. \end{cases} \tag{21}$$

In order to finish the proof of this theorem, we need to show that

$$\|\mathbb{P}^+ e_u^n\| \le C(h^{k+1} + \tau^2), \tag{22}$$

then using (21), the triangle inequality and the property (5), we can finish the proof of the theorem.

Combining (11) with (12) and using (21), by calculating we obtain that

$$\begin{aligned}
&\int_\Omega \mathbb{P}^+ e_u^n v dx + \lambda\beta \left\{ \int_\Omega \mathbb{P}^- e_q^n v_x dx - \sum_{i=1}^M \left[\left(\left(\mathbb{P}^- e_q^n\right)^- v^- \right)_{i+\frac{1}{2}} - \left(\left(\mathbb{P}^- e_q^n\right)^- v^+ \right)_{i-\frac{1}{2}} \right] \right\} \\
&\quad + \int_\Omega \mathbb{P}^- e_q^n \omega dx + \int_\Omega \mathbb{P}^+ e_u^n \omega_x dx - \sum_{i=1}^M \left\{ \left(\left(\mathbb{P}^+ e_u^n\right)^+ \omega^- \right)_{i+\frac{1}{2}} - \left(\left(\mathbb{P}^+ e_u^n\right)^+ \omega^+ \right)_{i-\frac{1}{2}} \right\} \\
&= \int_\Omega \left[\mathbb{P}^+ u(x,t_n) - u(x,t_n) \right] v dx \\
&\quad + \lambda\beta \left\{ \int_\Omega \left[\mathbb{P}^- q(x,t_n) - q(x,t_n) \right] v_x dx - \sum_{i=1}^M \left[\left(\left(\mathbb{P}^- q(x,t_n) - q(x,t_n) \right)^- v^- \right)_{i+\frac{1}{2}} \right. \right. \\
&\qquad \left. \left. - \left(\left(\mathbb{P}^- q(x,t_n) - q(x,t_n) \right)^- v^+ \right)_{i-\frac{1}{2}} \right] \right\} \\
&\quad + \int_\Omega \left[\mathbb{P}^- q(x,t_n) - q(x,t_n) \right] \omega dx + \int_\Omega \left[\mathbb{P}^+ u(x,t_n) - u(x,t_n) \right] \omega_x dx \\
&\quad - \sum_{i=1}^M \left\{ \left((\mathbb{P}^+ u(x,t_n) - u(x,t_n))^+ \omega^- \right)_{i+\frac{1}{2}} - \left((\mathbb{P}^+ u(x,t_n) - u(x,t_n))^+ \omega^+ \right)_{i-\frac{1}{2}} \right\} \\
&\quad + \sum_{j=2}^{n-1} (-b_j + 2b_{j-1} - b_{j-2}) \int_\Omega \left\{ \mathbb{P}^+ e_u^{n-j} - [\mathbb{P}^+ u(x,t_{n-j}) - u(x,t_{n-j})] \right\} v dx \\
&\quad + (2b_{n-1} - b_{n-2}) \int_\Omega \left\{ \mathbb{P}^+ e_u^0 - [\mathbb{P}^+ u(x,t_0) - u(x,t_0)] \right\} v dx - b_{n-1} \int_\Omega e_u^{-1} v dx \\
&\quad + (2b_0 - b_1) \int_\Omega \left\{ \mathbb{P}^+ e_u^{n-1} - [\mathbb{P}^+ u(x,t_{n-1}) - u(x,t_{n-1})] \right\} v dx - \beta \int_\Omega E_\tau^n(x) v dx.
\end{aligned} \tag{23}$$

Taking $v = \mathbb{P}^+ e_u^n$ and $\omega = \lambda\beta\mathbb{P}^- e_q^n$ in (23), and using the properties (4), we can get the following result,

$$
\begin{aligned}
&\int_\Omega \left(\mathbb{P}^+ e_u^n\right)^2 dx + \lambda\beta \int_\Omega \left(\mathbb{P}^- e_q^n\right)^2 dx \\
&\quad = \int_\Omega \left[\mathbb{P}^+ u(x,t_n) - u(x,t_n)\right]\mathbb{P}^+ e_u^n dx \\
&\qquad - \lambda\beta \sum_{i=1}^{M} \Big\{ \left\{[\mathbb{P}^- q(x,t_n) - q(x,t_n)]^- \left(\mathbb{P}^+ e_u^n\right)^-\right\}_{i+\frac{1}{2}} \\
&\qquad\qquad - \left\{[\mathbb{P}^- q(x,t_n) - q(x,t_n)]^- \left(\mathbb{P}^+ e_u^n\right)^+\right\}_{i-\frac{1}{2}} \Big\} \\
&\qquad + \lambda\beta \int_\Omega \left[\mathbb{P}^- q(x,t_n) - q(x,t_n)\right]\mathbb{P}^- e_q^n dx \\
&\qquad - \lambda\beta \sum_{i=1}^{M} \Big\{ \left\{[\mathbb{P}^+ u(x,t_n) - u(x,t_n)]^+ \left(\mathbb{P}^- e_q^n\right)^-\right\}_{i+\frac{1}{2}} \\
&\qquad\qquad - \left\{\left[\mathbb{P}^+ u(x,t_n) - u(x,t_n)\right]^+ \left(\mathbb{P}^- e_q^n\right)^+\right\}_{i-\frac{1}{2}} \Big\} \\
&\qquad + \sum_{j=2}^{n-1} \left(-b_j + 2b_{j-1} - b_{j-2}\right) \\
&\qquad \times \int_\Omega \left\{\mathbb{P}^+ e_u^{n-j} - [\mathbb{P}^+ u(x,t_{n-j}) - u(x,t_{n-j})]\right\}\mathbb{P}^+ e_u^n dx \\
&\qquad + (2b_{n-1} - b_{n-2}) \int_\Omega \left\{\mathbb{P}^+ e_u^0 - [\mathbb{P}^+ u(x,t_0) - u(x,t_0)]\right\}\mathbb{P}^+ e_u^n dx \\
&\qquad - b_{n-1} \int_\Omega e_u^{-1}\mathbb{P}^+ e_u^n dx \\
&\qquad + (2b_0 - b_1) \int_\Omega \left\{\mathbb{P}^+ e_u^{n-1} - [\mathbb{P}^+ u(x,t_{n-1}) - u(x,t_{n-1})]\right\}\mathbb{P}^+ e_u^n dx \\
&\qquad - \beta \int_\Omega E_\tau^n(x) v dx. \qquad (24)
\end{aligned}
$$

By (24) and the fact that $AB \le \frac{1}{2}A^2 + \frac{1}{2}B^2$, the following inequality holds,

$$
\begin{aligned}
&\|\mathbb{P}^+ e_u^n\|^2 + \lambda\beta\|\mathbb{P}^- e_q^n\|^2 \\
&\quad \le \Big\{\|\mathbb{P}^+ u(x,t_n) - u(x,t_n)\| + \sum_{j=2}^{n-1} |-b_j + 2b_{j-1} - b_{j-2}|\|\mathbb{P}^+ e_u^{n-j}\| \\
&\qquad + \sum_{j=2}^{n-1} |-b_j + 2b_{j-1} - b_{j-2}|\|\mathbb{P}^+ u(x,t_{n-j}) - u(x,t_{n-j})\|
\end{aligned}
$$

$$
\begin{aligned}
&+ |2b_{n-1} - b_{n-2}| \|\mathbb{P}^+ e_u^0\| + |2b_{n-1} - b_{n-2}| \|\mathbb{P}^+ u(x,t_0) - u(x,t_0)\| \\
&+ b_{n-1} \|e_u^{-1}\| + (2b_0 - b_1) \|\mathbb{P}^+ e_u^{n-1}\| \\
&+ (2b_0 - b_1) \|\mathbb{P}^+ u(x,t_{n-1}) - u(x,t_{n-1})\| \\
&+ \beta \|E_\tau^n(x)\| \Big\} \|\mathbb{P}^+ e_u^n\| + \lambda\beta \|\mathbb{P}^- q(x,t_n) - q(x,t_n)\| \|\mathbb{P}^- e_q^n\| \\
\le\ & \frac{1}{2} \Big\{ \|\mathbb{P}^+ u(x,t_n) - u(x,t_n)\| + \sum_{j=2}^{n-1} |-b_j + 2b_{j-1} - b_{j-2}| \|\mathbb{P}^+ e_u^{n-j}\| \\
&+ \sum_{j=2}^{n-1} |-b_j + 2b_{j-1} - b_{j-2}| \|\mathbb{P}^+ u(x,t_{n-j}) - u(x,t_{n-j})\| \\
&+ |2b_{n-1} - b_{n-2}| \|\mathbb{P}^+ e_u^0\| + |2b_{n-1} - b_{n-2}| \|\mathbb{P}^+ u(x,t_0) - u(x,t_0)\| \\
&+ b_{n-1} \|e_u^{-1}\| + (2b_0 - b_1) \|\mathbb{P}^+ e_u^{n-1}\| \\
&+ (2b_0 - b_1) \|\mathbb{P}^+ u(x,t_{n-1}) - u(x,t_{n-1})\| \\
&+ \beta \|E_\tau^n(x)\| \Big\}^2 + \frac{1}{2} \|\mathbb{P}^+ e_u^n\|^2 \\
&+ \frac{1}{2} \lambda\beta \|\mathbb{P}^- q(x,t_n) - q(x,t_n)\|^2 + \frac{1}{2} \lambda\beta \|\mathbb{P}^- e_q^n\|^2,
\end{aligned}
\tag{25}
$$

which means that

$$
\begin{aligned}
&\|\mathbb{P}^+ e_u^n\|^2 \\
&\le \Bigg\{ \|\mathbb{P}^+ u(x,t_n) - u(x,t_n)\| + \sum_{j=2}^{n-1} |-b_j + 2b_{j-1} - b_{j-2}| \|\mathbb{P}^+ e_u^{n-j}\| \\
&\quad + \sum_{j=2}^{n-1} |-b_j + 2b_{j-1} - b_{j-2}| \|\mathbb{P}^+ u(x,t_{n-j}) - u(x,t_{n-j})\| \\
&\quad + |2b_{n-1} - b_{n-2}| \|\mathbb{P}^+ e_u^0\| + |2b_{n-1} - b_{n-2}| \|\mathbb{P}^+ u(x,t_0) - u(x,t_0)\| \\
&\quad + b_{n-1} \|e_u^{-1}\| + (2b_0 - b_1) \|\mathbb{P}^+ e_u^{n-1}\| \\
&\quad + (2b_0 - b_1) \|\mathbb{P}^+ u(x,t_{n-1}) - u(x,t_{n-1})\| + \beta \|E_\tau^n(x)\| \Bigg\}^2 \\
&\quad + \lambda\beta \|\mathbb{P}^- q(x,t_n) - q(x,t_n)\|^2.
\end{aligned}
\tag{26}
$$

Next, we use mathematical induction to get the error estimation,

$$
\|\mathbb{P}^+ e_u^n\|^2 \le C^2 (h^{k+1} + \tau^2)^2. \tag{27}
$$

Similar to Lemma 3.2, we can also use mathematical induction to prove the inequality (27). When $n = 1$, by (10), the property (5) and the fact that h^{k+1} is lower than $\tau^{\frac{\alpha}{2}} h^{k+1}$, we have

$$\begin{aligned}\|\mathbb{P}^+ e_u^1\|^2 &\le \Big\{\|\mathbb{P}^+ u(x,t_1) - u(x,t_1)\| + 2\|\mathbb{P}^+ e_u^0\| + 2\|\mathbb{P}^+ u(x,t_0) - u(x,t_0)\| \\ &\qquad + \|e_u^{-1}\| + \beta\|E_\tau^n(x)\|\Big\}^2 + \lambda\beta\|\mathbb{P}^- q(x,t_n) - q(x,t_n)\|^2 \\ &\le C^2(h^{k+1} + \tau^2)^2 + C^2(\tau^{\frac{\alpha}{2}} h^{k+1})^2 \\ &\le C^2(h^{k+1} + \tau^2)^2. \end{aligned} \tag{28}$$

Assuming that $\|\mathbb{P}^+ e_u^n\|^2 \le C^2(h^{k+1} + \tau^2)^2$ holds for $n = J (J < N)$, we want to prove that it holds for $n = J + 1$. For $n = J + 1$, by the inequality (26) we get that

$$\begin{aligned}&\|\mathbb{P}^+ e_u^{J+1}\|^2 \\ &\le \Bigg\{\|\mathbb{P}^+ u(x,t_{J+1}) - u(x,t_{J+1})\| + \sum_{j=2}^{J} |-b_j + 2b_{j-1} - b_{j-2}|\|\mathbb{P}^+ e_u^{J+1-j}\| \\ &\qquad + \sum_{j=2}^{J} |-b_j + 2b_{j-1} - b_{j-2}|\|\mathbb{P}^+ u(x,t_{J+1-j}) - u(x,t_{J+1-j})\| \\ &\qquad + |2b_J - b_{J-1}|\|\mathbb{P}^+ e_u^0\| + |2b_J - b_{J-1}|\|\mathbb{P}^+ u(x,t_0) - u(x,t_0)\| \\ &\qquad + b_J\|e_u^{-1}\| + (2b_0 - b_1)\|\mathbb{P}^+ e_u^J\| + \beta\|E_\tau^{J+1}(x)\| \\ &\qquad + (2b_0 - b_1)\|\mathbb{P}^+ u(x,t_J) - u(x,t_J)\|\Big\}^2 + \lambda\beta\|\mathbb{P}^- q(x,t_{J+1}) - q(x,t_{J+1})\|^2. \\ &\le C^2\Bigg\{\Bigg[\sum_{j=2}^{J}(b_{j-2} - b_j) + b_J + (2b_0 - b_1)\Bigg](h^{k+1} + \tau^2) \\ &\qquad + \Bigg[\sum_{j=2}^{J}(b_{j-2} - b_j) + 2b_{J-1} + 3b_0 - b_1\Bigg]h^{k+1} + \tau^{\alpha+1}\Bigg\}^2 \\ &\qquad + C^2\left(\tau^{\frac{\alpha}{2}} h^{k+1}\right)^2. \end{aligned} \tag{29}$$

We know that τ^2 is lower than $\tau^{\alpha+1}$ because of $1 < \alpha \le 2$. Since $0 < b_j < 1$ for all non-negative integers j, then (29) will become

$$\|\mathbb{P}^+ e_u^{J+1}\|^2 \le C^2\big[(h^{k+1} + \tau^2)\big]^2. \tag{30}$$

So we have completed the proof of (22) and the proof is completed. □

Table 1 The error, L^2 space convergence rates (the fourth column) and L^∞ space convergence rates (the last column) of Example 1 for $\tau = 0.5h^3$ and using piecewise P^0 elements

α	M	L^2-error	Rate	L^∞-error	Rate
1.2	5	1.49933e-004	–	4.08359e-004	–
	10	7.18084e-005	1.0621	2.02277e-004	1.0135
	15	4.74981e-005	1.0194	1.35798e-004	0.9828
	20	3.55254e-005	1.0096	1.01879e-004	0.9982
1.6	5	1.48925e-004	–	4.10518e-004	–
	10	7.17460e-005	1.0536	2.01945e-004	1.0235
	15	4.74837e-005	1.0180	1.36016e-004	0.9747
	20	3.55212e-005	1.0089	1.02010e-004	1.0001
1.9	5	1.48266e-004	–	4.16165e-004	–
	10	7.17234e-005	1.0477	2.01914e-004	1.0434
	15	4.74865e-005	1.0170	1.36502e-004	0.9656
	20	3.55324e-005	1.0081	1.02071e-004	1.0104

4 Numerical examples

In this section, we carry out a series of numerical experiments and present some results to confirm our theoretical statements. Taking $h = 1/M$ and $\tau = 1/N$, where M and N are the numbers of meshes in space and time. The L^2-norm and L^∞-norm are considered in the examples.

Example 1 We consider the following homogeneous boundary condition problem

$$\begin{cases} D_t^\alpha u(x,t) - t\Delta u(x,t) = f(x,t), \quad (x,t) \in [0,1] \times [0,1], \\ u(0,t) = u(1,t) = 0, \ u(x,t)\,|_{t=0} = 0, \ \dfrac{\partial u(x,t)}{\partial t}\,|_{t=0} = 0, \end{cases} \tag{31}$$

with $f(x,t) = \frac{6}{\Gamma(4-\alpha)} t^{(3-\alpha)}(x-x^2)^5 - t^4(20x^3 - 150x^4 + 420x^5 - 560x^6 + 360x^7 - 90x^8)$.

Table 2 The error, L^2 space convergence rates (the fourth column) and L^∞ space convergence rates (the last column) of Example 1 for $\tau = 0.5h^3$ and using piecewise P^1 elements

α	M	L^2-error	Rate	L^∞-error	Rate
1.2	5	4.68571e-005	–	2.22760e-004	–
	10	1.19892e-005	1.9665	6.03418e-005	1.8843
	15	5.34284e-006	1.9934	2.85046e-005	1.8496
	20	3.00808e-006	1.9968	1.59916e-005	2.0092
1.6	5	4.67894e-005	–	2.22515e-004	–
	10	1.19863e-005	1.9648	6.03203e-005	1.8832
	15	5.34224e-006	1.9931	2.84962e-005	1.8495
	20	3.00786e-006	1.9967	1.59854e-005	2.0095
1.9	5	4.67871e-005	–	2.22954e-004	–
	10	1.19870e-005	1.9646	6.03856e-005	1.8845
	15	5.34234e-006	1.9932	2.85151e-005	1.8505
	20	3.00787e-006	1.9968	1.59921e-005	2.0103

Table 3 The error, L^2 space convergence rates (the fourth column) and L^∞ space convergence rates (the last column) of Example 1 for $\tau = 0.5h^3$ and using piecewise P^2 elements

α	M	L^2-error	Rate	L^∞-error	Rate
1.2	5	7.65138e-006	–	4.01305e-005	–
	10	9.91877e-007	2.9475	5.83554e-006	2.7818
	15	2.98522e-007	2.9614	1.73026e-006	2.9983
	20	1.27160e-007	2.9665	7.25087e-007	3.0233
1.6	5	7.69466e-006	–	4.02426e-005	–
	10	9.93156e-007	2.9538	5.83652e-006	2.7855
	15	2.97754e-007	2.9710	1.72621e-006	3.0045
	20	1.26037e-007	2.9883	7.20372e-007	3.0378
1.9	5	8.05815e-006	–	4.11242e-005	–
	10	1.02954e-006	2.9684	5.93185e-006	2.7934
	15	3.06898e-007	2.9851	1.75063e-006	3.0098
	20	1.29304e-007	3.0045	7.29005e-007	3.0452

The exact solution of the problem is given by $u(x,t) = t^3(x-x^2)^5$. For this example we choose $\tau = 0.5h^3$. We used the elements P^0, P^1 and P^2 for the considered problem, respectively. The error estimate are presented in Tables 1, 2 and 3 for different M at given α. We can see from Tables 1–3 that the L^2-error and L^∞-error convergence rates for space yield the approximation order close to first-order, second-order and third-order for P^0, P^1 and P^2 elements, respectively, which confirm the theoretical prediction. For the time convergence rates, we only consider the P^1 elements. In Fig. 1a and b, we take $M = 500$ and $N = 50, 100, 200, 400$ for the time convergence rate, we can see from these figures that the time convergence rates are very close to the first-order. From Table 4, we can see that L^2-error convergence rates for time yield the approximation order close to first-order for P^1 elements. The time convergence rates are lower about one order than the theoretical prediction, that is because the space step is not small enough. However, if h is taken sufficiently small so that the error in the approximation should be dominated by the temporal approximation, the storage requirement to save the solution

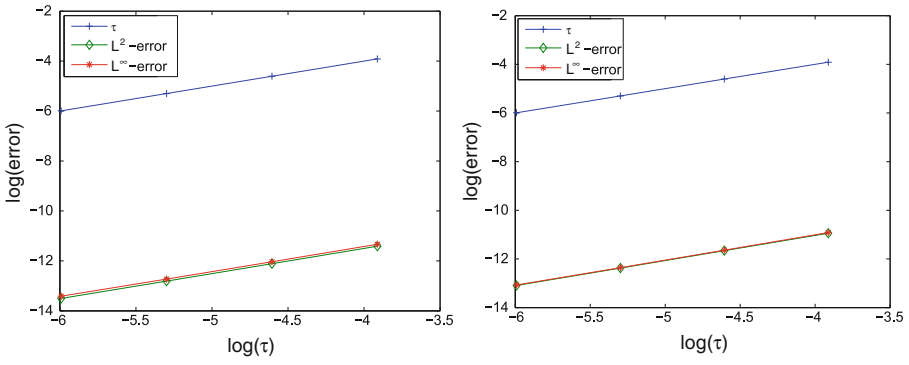

a. α = 1.2 b. α = 1.9

Fig. 1 The time convergence rates analysis of Example 1 with $M = 500$ for different α

Table 4 The error, L^2 time convergence rates of Example 1 for $M = 500$ and using piecewise P^1 elements

α	N	L^2-error	Rate	α	N	L^2-error	Rate
1.2	50	1.10563e-005	–	1.9	50	1.76945e-005	–
	100	5.48620e-006	1.0110		100	8.65034e-006	1.0324
	200	2.73205e-006	1.0058		200	4.22448e-006	1.0340
	400	1.36432e-006	1.0018		400	2.06272e-006	1.0342

for all time levels may not be acceptable in practical applications. In our future works, we will pay more attention to construct efficient algorithms to reduce the storage requirement.

Example 2 In this example, we will consider the following periodic boundary condition problem

$$\begin{cases} D_t^{\alpha} u(x,t) - t^2 \Delta u(x,t) = f(x,t), \quad (x,t) \in [0,1] \times [0,1], \\ u(0,t) = u(1,t) = 1, \ u(x,t)\,|_{t=0} = 0, \ \dfrac{\partial u(x,t)}{\partial t}\,|_{t=0} = 0, \end{cases} \tag{32}$$

with $f(x,t) = (\frac{6}{\Gamma(4-\alpha)} t^{(3-\alpha)} + 4\pi^2 t^5)\cos(2\pi x)$.

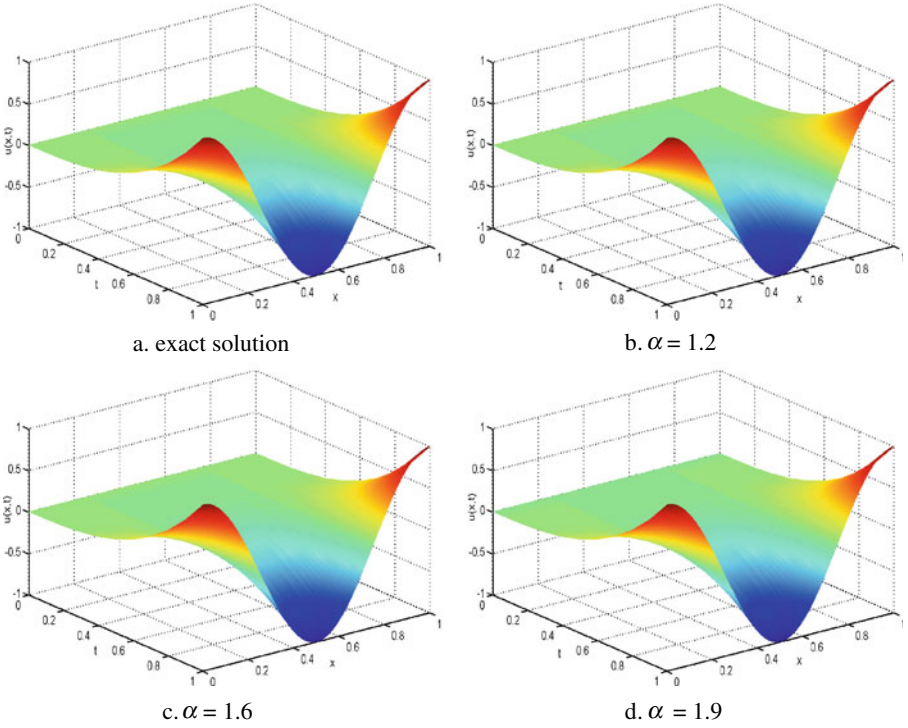

a. exact solution b. $\alpha = 1.2$ c. $\alpha = 1.6$ d. $\alpha = 1.9$

Fig. 2 The exact solution and LDG numerical solutions of Example 2 for different α at $N = 1{,}000$ and $M = 30$

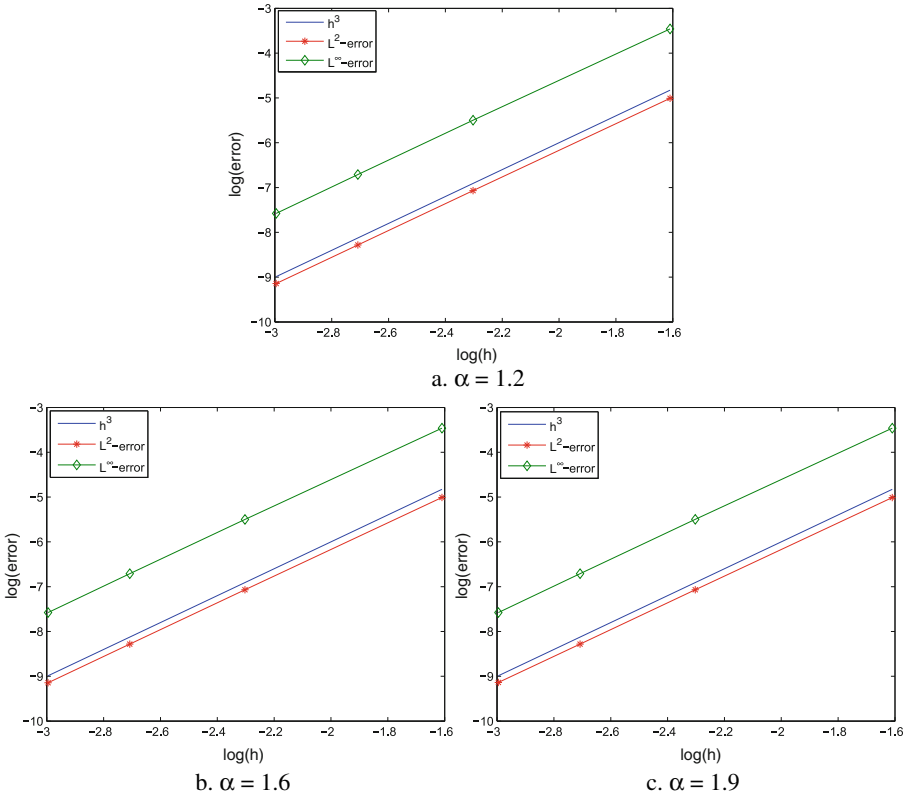

Fig. 3 The space convergence rates analysis of Example 2 with $N = 10{,}000$ for different α

The exact solution of the problem is $u(x,t) = t^3\cos(2\pi x)$. We used the elements P^2 for the considered problem. Figure 2a–d show the exact solution and LDG numerical solutions of Example 2 for different α at given $M = 30$ and $N = 1{,}000$. We can see from these figures that the numerical solutions are almost the same, because the exact solution is the same one for different α. In Fig. 3a–c, we take $N = 10{,}000$ and $M = 5, 10, 15, 20$ for the space convergence rate, we can see from these figures that the space convergence rates are very close to the third-order. The numerical results for the problem are consistent with our theoretical analysis.

Table 5 The error, L^2 space convergence rates (the fourth column) and L^∞ space convergence rates (the last column) of Example 3 for $\tau = 0.5h^3$ and using piecewise P^0 elements

α	M	L^2-error	Rate	L^∞-error	Rate
2	5	4.36479e-001	–	6.98686e-001	–
	10	1.51684e-001	1.5248	3.19793e-001	1.1275
	15	9.22909e-002	1.2254	2.10735e-001	1.0286
	20	6.73199e-002	1.0967	1.57829e-001	1.0049

Table 6 The error, L^2 space convergence rate (the fourth column) and L^∞ space convergence rate (the last column) of Example 3 for $\tau = 0.5h^3$ and using piecewise P^2 elements

α	M	L^2-error	Rate	L^∞-error	Rate
2	5	5.50223e-002	–	8.08142e-002	–
	10	7.00770e-003	2.9730	9.96147e-003	3.0202
	15	2.09129e-003	2.9823	3.01571e-003	2.9470
	20	8.77750e-004	3.0178	1.26621e-003	3.0165

Example 3 In this example, in order to verify the validity of LDG method, we will consider the following time-fractional wave equation

$$\begin{cases} D_t^\alpha u(x,t) - \Delta u(x,t) = 0, \quad (x,t) \in [0,1] \times [0,1], \\ u(0,t) = u(1,t) = 0, \ u(x,t)\,|_{t=0} = \sin(2\pi x), \ \dfrac{\partial u(x,t)}{\partial t}\,|_{t=0} = 2\pi \sin(2\pi x). \end{cases} \tag{33}$$

For $\alpha = 2$, (33) will become the classical wave equation. The exact solution of the classical wave equation is given by $u(x,t) = \sin(2\pi x)(\sin(2\pi t) + \cos(2\pi t))$. We used the elements P^0 and P^2 for the considered problem,

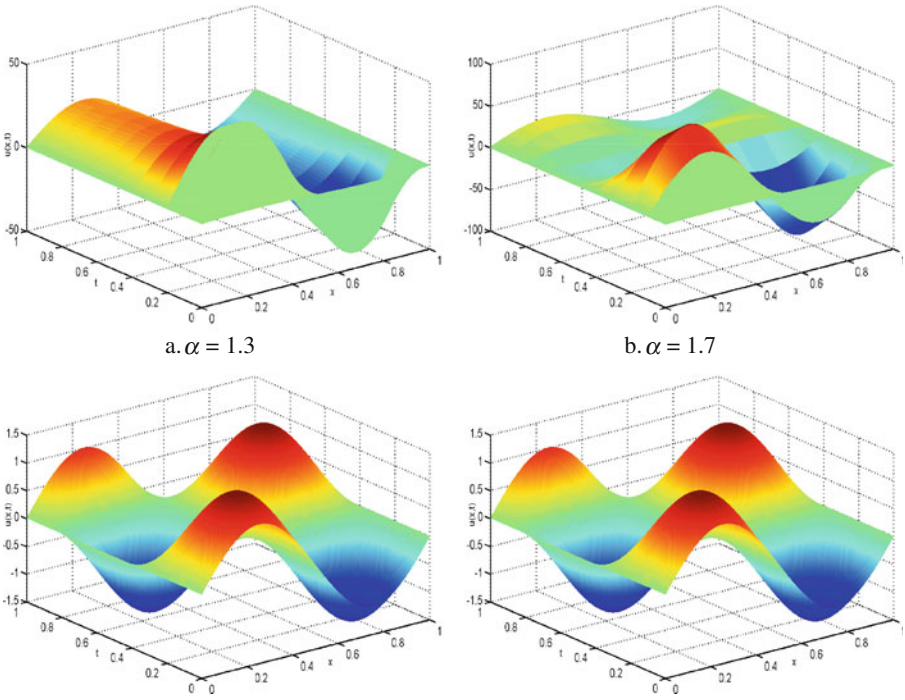

a. $\alpha = 1.3$ b. $\alpha = 1.7$

c. The numerical solution for $\alpha = 2$ d. The exact solution for $\alpha = 2$

Fig. 4 The exact solution and LDG numerical solutions of Example 3 for different α at $N = 1{,}000$ and $M = 50$

respectively. If we choose $\tau = 0.5h^3$, the error estimates are presented in Tables 5 and 6 for different M at $\alpha = 2$. We can see from Tables 5 and 6 that the L^2-error and L^∞-error convergence rates for space yield the approximation order close to first-order and third-order for P^0 and P^2 elements, respectively, which confirm the theoretical prediction. For P^2 elements, Fig. 4a–d show the exact solution and LDG numerical solutions of Example 3 for different α at given $M = 50$ and $N = 1{,}000$. We can see from these figures that there are great difference for numerical solutions of different α, because the exact solution is the not the same one for different α. Figure 4a and b show that for $1 < \alpha < 2$, the considered problem exhibits the combined diffusion and wave behaviour (It should be pointed out that the exact solution is difficult to be obtained for $1 < \alpha < 2$, therefore, it is difficult to get the convergence rates). However, from Fig. 4c and d we can find that the numerical solution is good approximation of the exact solution for $\alpha = 2$, which means that our method is effective.

5 Conclusion

In this paper, we have developed local discontinuous Galerkin methods to solve the one-dimensional time-fractional Tricomi-type equations. The stability analysis and error estimates for the full discrete scheme is discussed. Numerical examples for one-dimensional cases are given to illustrate the accuracy and capability of the methods. The LDG method has a good potential in solving the one-dimensional time-fractional Tricomi-type equations and similar linear or nonlinear equations in mathematical physics. This idea can be also used for two-dimensional fractional problems. However, in three-dimensional case the storage requirement to save the solution for all time levels may not be acceptable in practical applications. Constructing more efficient algorithms to reduce the storage requirement is also our goal in future works. Future work also includes the proof of convergence for general P^k polynomials when using a non-uniform grid and the exploration of higher-order nonlinear equations.

Acknowledgements The authors would like to thank the anonymous referees for their valuable suggestion and comments which have improved the paper.

References

1. Miller, K.S., Ross, B.: An Introduction to the Fractional Calculus and Fractional Differential Equations. Wiley, New York (1993)
2. He, J.H.: Nonlinear oscillation with fractional derivative and its applications. In: International Conference on Vibrating Engineering'98. Dalian, China, pp. 288–291 (1998)
3. He, J.H.: Some applications of nonlinear fractional differential equations and their approximations. Bull Sci Technol. **15**, 86–90 (1999)

4. He, J.H.: Approximate analytical solution for seepage flow with fractional derivatives in porous media. Comput. Methods Appl. Mech. Eng. **167**, 57–68 (1998)
5. Mainardi, F.: Fractional calculus, some basic problems in continuum and statistical mechanics. In: Carpinteri, A., Mainardi, F., (eds.) Fractals and Fractional Calculus in Continuum Mechanics, pp. 291–348. Springer, Wien (1997)
6. Podlubny, I.: Fractional Differential Equations. Academic Press, New York (1999)
7. Kemppainen, J.T., Ruotsalainen, K.M.: On the spline collocation method for the single layer equation related to time-fractional diffusion. Numer. Algorithms **57** 313–327 (2011)
8. Shen, S.J., Liu, F.W., Anh, V.: Numerical approximations and solution techniques for the space-time Riesz–Caputo fractional advection-diffusion equation. Numer. Algorithms **56**, 383–403 (2011)
9. Chen, S., Liu, F.W., Anh, V.: A novel implicit finite difference method for the one-dimensional fractional percolation equation. Numer. Algorithms **56** 517–535 (2011)
10. Lin, Y.M., Xu, C.J.: Finite difference/spectral approximations for the time-fractional diffusion equation. J. Comput. Phys. **225**, 1533–1552 (2007)
11. Tadjeran, C., Meerschaert, M.M.: A second-order accurate numerical method for the two-dimensional fractional diffusion equation. J. Comput. Phys. **220**, 813–823 (2007)
12. Meerschaert, M.M., Tadjeran, C.: Finite difference approximations for two-sided space-fractional partial differential equations. Appl. Numer. Math. **56**(1), 80–90 (2006)
13. Meerschaert, M.M., Scheffler, H.P., Tadjeran, C.: Finite difference methods for two-dimensional fractional dispersion equation. J. Comput. Phys. **211**, 249–261 (2006)
14. Yuste, S.B., Acedo, L.: An explicit finite difference method and a new von Numann-type stability analysis for fractional diffusion equations. SIAM J. Numer. Anal. **42**, 1862–1874 (2005)
15. Meerschaert, M.M., Tadjeran, C.: Finite difference approximations for fractional advection–dispersion flow equations. J. Comput. Appl. Math. **172**, 65–77 (2004)
16. Meerschaert, M.M., Benson, D.A., Baeumer, B.: Multidimensional advection and fractional dispersion. Phys. Rev. E. **59**, 5026–5028 (1999)
17. Podlubny, I.: The Laplace Transform Method for Linear Differential Equations of Fractional Order. Slovac Academy of Science, Slovak Republic (1994)
18. Nawaz, Y.: Variational iteration method and homotopy perturbation method for fourth-order fractional integro-differential equations. Comput. Math. Appl. **61**, 2330–2341 (2011)
19. Luchko, Y., Srivastava, H.: The exact solution of certain differential equations of fractional order by using operational calculus. Comput. Math. Appl. **29**, 73–85 (1995)
20. Cveticanin, L.: Homotopy perturbation method for pure nonlinear differential equation. Chaos, Solitons Fractals **30**, 1221–1230 (2006)
21. Rajabi, A., Ganji, D.D., Taherian, H.: Application of homotopy perturbation method in nonlinear heat conduction and convection equations. Phys. Lett. A **360**, 570–573 (2007)
22. Feng, X.L., Mei, L.Q., He, G.L.: An efficient algorithm for solving Troesch's problem. Appl. Math. Comput. **189**, 500–507 (2007)
23. Momani, S., Odibat, Z.: Homotopy perturbation method for nonlinear partial differential equations of fractional order. Phys. Lett. A **365**, 345–350 (2007)
24. Ganji, Z.Z., Ganji, D.D., Jafari, H., et al.: Application of the homotopy perturbation method to coupled system of partial differential equations with time fractional derivatives. Topol. Methods Nonlinear Anal. **31**, 341–348 (2008)
25. Yıldırım, A., Hüseyin, K.: Homotopy perturbation method for solving the space-time fractional advection-dispersion equation. Adv. Water Resour. **32**, 1711–1716 (2009)
26. Jafari, H., Golbabai, A., Seifi, S., Sayevand, K.: Homotopy analysis method for solving multi-term linear and nonlinear diffusion wave equations of fractional order. Comput. Math. Appl. **59**, 1337–1344 (2010)
27. Elsaid, A.: Homotopy analysis method for solving a class of fractional partial differential equations. Commun. Nonlinear Sci. Numer. Simul. **16**(9), 3655–3664 (2011)
28. Zhang, X.D., Tang, B., He, Y.N.: Homotopy analysis method for higher-order fractional integro-differential equations. Comput. Math. Appl. **62**, 3194–3203 (2011)
29. Tricomi, F.: Sulle equazioni lineari alle derivate parziali di secondo ordine, di tipo misto. Rend. R. Accad. Lincei, Cl. Sci. Fis. Mat. Natur. **5**(14), 134–247 (1923)
30. Frankl, F.: On the problems of Chaplygin for mixed sub- and supersonic flows. Bull. Acad. Sci. USSR Ser. Math. **9**, 121–143 (1945)

31. Bers, L.: Mathematical aspects of subsonic and transonic gas dynamics. In: Surveys in Applied Mathematics, vol. 3. Wiley/Chapman & Hall, New York/London (1958)
32. Cole, J.D., Cook, L.P.: Transonic Aerodynamics. Elsevier/North-Holland, Amsterdam/New York (1986)
33. Germain, P.: The Tricomi equation, its solutions and their applications in fluid dynamics. In: Tricomi's Ideas and Contemporary Applied Mathematics, Rome/Turin (1997). In: Atti Convegni Lincei, vol. 147, pp. 7–26. Accad. Naz. Lincei, Rome (1998)
34. Morawetz, C.: Mixed equations and transonic flow. J. Hyperbol Differ. Eq. **1**(1), 1–26 (2004)
35. Nocilla, S.: Applications and developments of the Tricomi equation in the transonic aerodynamics. In: Mixed Type Equations, Teubner-Texte Math., vol. 90, pp. 216–241. Teubner, Leipzig (1986)
36. Reed, W.H., Hill, T.R.: Triangular mesh methods for the neutron transport equation. Tech. Report LA-UR-73-479, Los Alamos Scientific Laboratory (1973)
37. Cockburn, B., Lin, S.-Y., Shu, C.-W.: TVB Runge-Kutta local projection discontinuous Galerkin finite element method for conservation laws III: one dimensional systems. J. Comput. Phys. **84**, 90–113 (1989)
38. Cockburn, B., Hou, S., Shu, C.-W.: The Runge-Kutta local projection discontinuous Galerkin finite element method for conservation laws IV: the multidimensional case. Math. Comput. **54**, 545–581 (1990)
39. Cockburn, B., Shu, C.-W.: The Runge–Kutta local projection P1-discontinuous-Galerkin finite element method for scalar conservation laws. Math. Model. Numer. Anal. (M2AN) **25**, 337–361 (1991)
40. Cockburn, B., Shu, C.-W.: The Runge–Kutta discontinuous Galerkin method for conservation laws V: multidimensional systems. J. Comput. Phys. **141**, 199–224 (1998)
41. Cockburn, B., Shu, C.-W.: The local discontinuous Galerkin method for timedependent convection diffusion systems. SIAM J. Numer. Anal. **35**, 2440–2463 (1998)
42. Cockburn, B., Kanschat, G., Perugia, I., Schotzau, D.: Superconvergence of the local discontinuous Galerkin method for elliptic problems on Cartesian grids. SIAM J. Numer. Anal. **39**, 264–285 (2001)
43. Yan, J., Shu, C.-W.: A local discontinuous Galerkin method for KdV type equations. SIAM J. Numer. Anal. **40**, 769–791 (2002)
44. Levy, D., Shu, C.-W., Yan, J.: Local discontinuous Galerkin methods for nonlinear dispersive equations. J. Comput. Phys. **196**, 751–772 (2004)
45. Xu, Y., Shu, C.-W.: Local discontinuous Galerkin methods for nonlinear Schrödinger equations. J. Comput. Phys. **205**, 72–97 (2005)
46. Xu, Y., Shu, C.-W.: Local discontinuous Galerkin method for the Camassa–Holm equation. SIAM J. Numer. Anal. **46**, 1998–2021 (2008)
47. Castillo, P.E.: Stencil reduction algorithms for the Local Discontinuous Galerkin method. Int. J. Numer. Methods Eng. **81**, 1475–1491 (2010)
48. Shao, L., Feng, X.L., He, Y.N.: The local discontinuous Galerkin finite element method for Burger's equation. Math. Comput. Model. **54**, 2943–2954 (2011)
49. Mustapha, K.: The hp- and h-versions of the discontinuous and local discontinuous Galerkin methods for one-dimensional singularly perturbed models. Appl. Numer. Math. **61**, 1223–1236 (2011)
50. Castillo, P., Sequeira, F.A.: Computational aspects of the local discontinuous Galerkin method on unstructured grids in three dimensions. Math. Comput. Model. (2011). doi:10.1016/j.mcm.2011.07.032
51. Cockburn, B., Dawson, C.: Some extensions of the local discontinuous Galerkin method for convection-diffusion equations in multidimensions. In: Whiteman, J. (ed.) Proceedings of the Conference on the Mathematics of Finite Elements and Applications: MAFELAP X, pp. 225–238. Elsevier (2000)
52. Castillo, P., Cockburn, B., Schötzau, D., Schwab, Ch.: Optimal a priori error estimates for the hp-version of the Local Discontinuous Galerkin method for convection-diffusion problems. Math. Comput. **71**, 455–478 (2001)
53. Castillo, P.: An optimal error estimate for the local discontinuous Galerkin method. In: Cockburn, B., Karniadakis, G.E., Shu, C.-W. (eds.) Discontinuous Galerkin Methods: Theory, Computation and Applications, Lectures Notes in Computational Science and Engineering, vol. 11, pp. 285–290. Springer (2000)

54. Wei, L.L., Zhang, X.D., He, Y.N.: Analysis of a local discontinuous Galerkin method for time-fractional advection-diffusion equations. Int. J. Numer. Methods Heat Fluid Flow (2012, in press)
55. Li, C.P., Zhao, Z.G., Chen, Y.Q.: Numerical approximation of nonlinear fractional differential equations with subdiffusion and superdiffusion. Comput. Math. Appl. **62**, 855–875 (2011)
56. Wei, L.L., He, Y.N., Zhang, X.D., Wang, S.L.: Analysis of an implicit fully discrete local discontinuous Galerkin method for the time-fractional Schrödinger equation. Finite Elem. Anal. Des. **59**, 28–34 (2012)